Simulation of the Delivery of Doxorubicin to Hepatoma

Yin-Min Felicia Goh,[1] Hwai Loong Kong,[2] and Chi-Hwa Wang[1,3]

Received January 2, 2001; accepted February 18, 2001

Purpose. To develop a two-dimensional simulation platform for the transport of doxorubicin to the hepatoma. To examine the temporal and spatial variation of doxorubicin concentration and its penetration into the tumor and the surrounding normal tissues.

Methods. Simulations are carried out with Fluent/UNS using the finite volume method to obtain the interstitial fluid pressure, velocity, and concentration profiles.

Results. Interstitial fluid pressure in the tumor and core reaches a steady state value in about 800 s, corresponding well with the assumed time scale for interstitial matrix fluid percolation (~1000 s). There is a strong correlation between the drug concentration in the interstitial space of tumor and blood plasma for time >> 1 h. Concentration of doxorubicin is highest in the viable zone of the tumor at early times and in the necrotic core at later times, and lowest in the surrounding normal tissues. Diffusion is the dominant form of transport for doxorubicin.

Conclusions. Varying the volume of solution injected, while keeping the dosage the same, does not cause significant changes in the amount and distribution of drug in the tumor. A higher vascular exchange area leads to higher concentrations of drug in the tumor. Lymphatic drainage in the tumor causes negligible reductions in the mean concentrations in all three different zones. Cellular metabolism and DNA binding kinetics decrease the mean concentrations of drug by about 15 to 40%, as compared to the baseline case.

KEY WORDS: doxorubicin; hepatoma; computer simulation; drug delivery; CFD.

INTRODUCTION

There are one million new cases of hepatoma worldwide each year. In many Asian countries it is a serious problem with as many as 150 cases per million population (1). Hepatomas are often not removed by surgery due to factors such as size and invasion into major vessels. For such cases, conservative therapies such as transcatheter arterial chemoembolization or arterial infusion chemotherapy are carried out.

Transcatheter oily chemoembolization is a process that treats hepatomas. The procedure involves the insertion of a catheter, about 50 cm long, through an opening in the groin of the patient into the hepatic artery or its branches. The tube is then guided up the artery until it reaches the hepatoma in the liver. The anticancer drug is mixed with lipiodol, an oily contrast medium, and is injected through the tube into the blood capillaries.

For treatment to be successful, the drug supplied by the blood vessels must pass through the microvascular wall into the interstitium of the tumor and travel through the interstitium to act on the cancer tissues. These transport processes involve both convection and diffusion. The high interstitial pressure found in the center of the tumor is a major physiologic barrier to drug delivery. Furthermore, the drug may be metabolized or degraded, hence reducing its efficacy.

Doxorubicin is an anthracycline antineoplastic agent used to treat a wide variety of tumors. Doxorubicin acts by completing with DNA, changing DNA conformation thus inhibiting DNA polymerase and protein synthesis. One of the drawbacks of doxorubicin treatment is its cardiotoxic effect. A cumulative dose of 550 mg/m^2 may cause heart failure. Hence, dosage must be carefully administered. Dosage is usually between 50 to 75 mg/m^2, administered in no less than 3 to 5 minutes (2) and is not repeated for three weeks. Intravenous infusion is not recommended because tissue damage may occur if doxorubicin infiltrates the tissue (2).

Netti *et al.* (3) examined the time-dependent behavior of interstitial fluid pressure and fluid pressure in tumors and studied ways to overcome the strong barrier posed by the elevated interstitial pressure to drug delivery in solid tumors. The effect of blood pressure modulation on macromolecular uptake in tumors was investigated (3,4). Their results showed that a higher uptake of macromolecules was possible through the periodic modulation of blood pressure and hence associated changes in the interstitial pressure. This enhanced delivery resulted from the increased transmural pressure gradient.

The aim of this study is to develop a two-dimensional simulation platform for the transport of doxorubicin to the hepatoma from the one-dimensional model by Baxter and Jain (5–8). Using this model, we can examine the temporal and spatial variation of doxorubicin concentration and its penetration into the tumor and the surrounding normal tissues. In addition, the effects of vascular exchange area, lymphatic drainage, intracellular kinetics on the concentration of doxorubicin are studied. This simulation model of drug delivery to tumors is proposed to help surgeons decide on the appropriate and optimal administration regimen for targeting the tumor cells.

MATHEMATICAL MODEL

This section presents the physiologic principles behind the transport of fluid and solute in tumor, together with the governing equations used in the simulations, primarily adapted from Baxter and Jain (5,6). The geometry used for the simulations is shown in Fig. 1a. It is generated from the CT scan of a hepatoma, as shown in Fig. 1b. The model consists of three domains: the necrotic core, viable tumor zone, and normal tissues. The necrotic core has no functional blood and lymphatic vessels. The viable tumor zone has partially functioning blood vessels but no lymphatic vessels, and the surrounding normal tissue has completely functional blood and lymphatic vessels. For simplicity, the necrotic core, viable tumor tissue, and normal tissue will henceforth be abbreviated as core, tumor, and tissue, respectively.

Interstitial Fluid Transport

Mass conservation for the interstitial fluid is given by the following equation:

[1] Department of Chemical and Environmental Engineering, National University of Singapore, 4 Engineering Drive 4, Singapore 117576.
[2] Department of Medicine, National University of Singapore, 10 Kent Ridge Crescent, Singapore 119260.
[3] To whom correspondence should be addressed. (e-mail: chewch@nus.edu.sg)

0724-8741/01/0600-0761$19.50/0

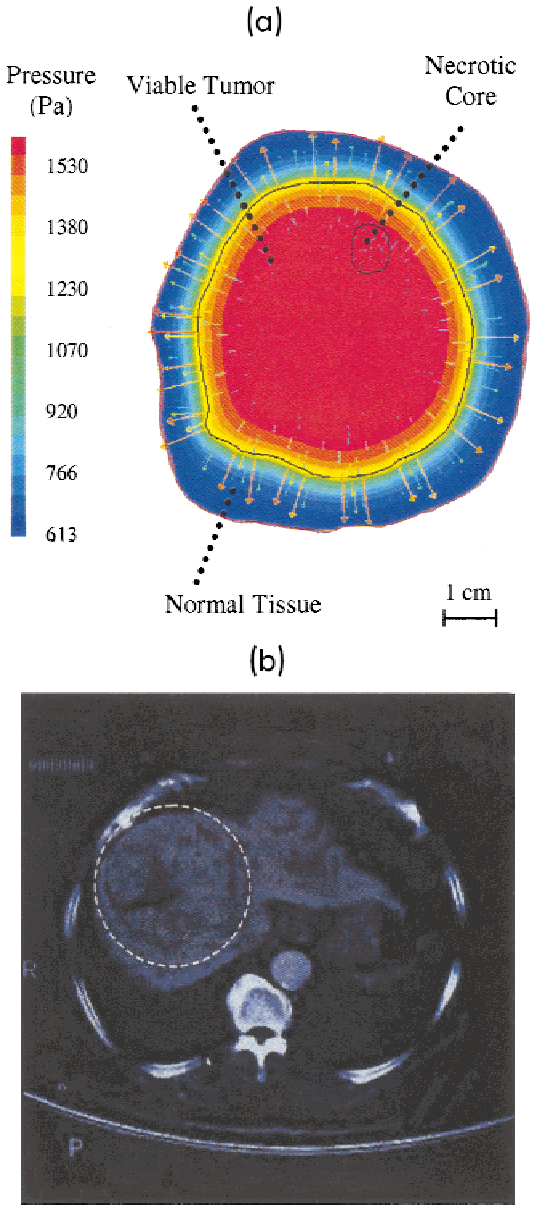

Fig. 1. (a) Computational geometry of hepatoma showing the interstitial pressure (P_i) distribution at steady-state. Arrows represent velocity vectors. Baseline parameter values are given in table 1. (b) CT scan of hepatoma.

$$\frac{\partial \rho}{\partial t} + \nabla \cdot (\rho v) = (F_v - F_l) \cdot \rho \tag{1}$$

where ρ is the density of the interstitial fluid, v is the fluid velocity, F_v is the interstitial fluid loss from the blood vessels per unit volume of tumor tissue, and F_1 is the fluid absorption rate by the lymphatics per unit volume of tumor tissue. The triangle (∇) refers to the symbol "divergence." The divergence of ρv represents the net mass flow rate of interstitial fluid per unit volume of tissue. F_v and F_1 are given by Starling's law (5,9):

$$F_v = K_v \frac{S}{V} [P_v - P_i - \sigma_T (\pi_v - \pi_i)] \tag{2}$$

where K_v is the hydraulic conductivity of the microvascular wall, S/V is the surface area of blood vessels per unit volume of tumor tissue, P_v is the vascular pressure, P_i is the interstitial pressure, σ_T is the average osmotic reflection coefficient for plasma proteins, and π_v and π_i are the osmotic pressures of the plasma and interstitial fluid, respectively.

Injection of the drug into the blood vessels will lead to an increase in P_v. It is taken to be a step increase, with the subsequent decay modeled as a decreasing exponential function:

$$P_v = P_{vo} [1 + A \exp(-t/tc)] \tag{3}$$

where A is the percentage increase in P_v due to injection of the drug and fluid (refer to appendix A) and tc is the time constant for the decay. The increase in vascular pressure is related to both the volume of fluid injection and the duration of injection. This has been incorporated in the present study by modeling the infusion of fluid into parallel capillaries (i.e. the microvascular bed). The lymphatic drainage term is taken to be proportional to the pressure difference between the interstitium and the lymphatics:

$$F_l = K_l \frac{S_l}{V} (P_i - P_l) \tag{4}$$

where K_l is the hydraulic conductivity of the lymphatic wall, S_l/V is the surface area of lymphatic vessels per unit volume of tumor tissue, and P_l is the intra-lymphatic pressure. The interstitium is modelled as a rigid porous medium, with the momentum equation given by (10):

$$\frac{\partial(\rho v)}{\partial t} + \nabla \cdot (\rho v v) = -\nabla P_i + [\nabla \cdot \Gamma] + \rho g + F \tag{5}$$

where Γ and g are the stress tensor and gravity acceleration. The additional term F counts for the Darcian resistance to fluid flow through porous media and is given by:

$$F = W \mu v + I \tfrac{1}{2} \rho | v | v \tag{6}$$

where μ is the dynamic viscosity of the interstitial fluid, W and I are the prescribed matrices of the viscous loss term and the inertial loss term respectively. For a homogeneous medium, W is a diagonal matrix with all diagonal elements given by $1/\kappa$, where κ is the permeability of the porous interstitium. In equation 5, the inertial loss term ($I \tfrac{1}{2} \rho | v | v$) can be neglected as compared with the Darcian resistance ($F = W \mu v$) upon recalling that the velocity of the interstitial fluid is very low ($| v | << 1$). In additional, the interstitial fluid is treated as incompressible with a constant viscosity value.

Solute Transport

Mass conservation of the drug is given by the following equation:

$$\frac{\partial(\rho m_i)}{\partial t} + \nabla \cdot (\rho m_i v) = -D\nabla^2 (\rho m_i) + R_i + S_i \tag{7}$$

where m_i is the mass fraction of the drug in the interstitium, D is the diffusion coefficient of the drug, and R_i is the mass rate of creation or depletion of the drug by intracellular kinetics. This can be attributed to either cellular metabolism (r_i) or bindings with DNA (B_i): $R_i = r_i + B_i$). The closures for m_i and B_i and their effects on the effective drug concentration will be described in the later sections "Effect of Cellular Metabolism" and "Doxorubicin-DNA Binding Kinetics," respec-

tively. The source term S_i is the net rate of drug gained from the blood vessels,

$$S_i = (F_s - F_{ls}) \cdot (\text{MW of drug}) \quad (8)$$

where F_s is the drug gain from the blood capillaries (in tumor and tissues); F_{ls} is the drug loss to the lymphatic vessels per unit volume of tissue. The rate of gain of drug from the blood vessels is given by (5,9):

$$F_s = F_v(1-\sigma)C_v + P\frac{S}{V}(C_v - C_i)\frac{Pe_v}{\exp(Pe_v) - 1} \quad (9)$$

where Pe_v, the transcapillary Peclet number, which is the ratio of convection to diffusion across the capillary wall is defined as:

$$Pe_v = \frac{F_v(1-\sigma)}{P\frac{S}{V}} \quad (10)$$

and σ is the osmotic reflection coefficient for the drug molecules, C_v is the concentration of drug in the blood plasma (depending on the dosage used), and P is the vascular permeability coefficient. The rate of drug loss by the lymphatics is given by (6):

$$F_{ls} = F_1 C_i \quad (11)$$

C_v is modeled as a decaying function of time (see appendix B). The arterial blood doxorubicin concentrations perfusing the normal tissue and the viable tumor are taken to be equal but time-dependent. The values of the parameters used for the baseline simulations are given in Table I. These parameters can be roughly classified into two categories: (i) physical and transport properties and (ii) kinetic parameters. Parameter values in the first category (S/V, K_v, K, tc, π_v, π_i, P, σ_T, and σ) are largely taken from the literature in which measurements have been collected through animal experiments for normal and tumor tissues separately. Parameters in the second category (C_{vo}, T_w, k*, and k_i) are mostly pharmacokinetic parameters. The transport and kinetic parameters are uniform in each computational domain (tumor, tissue, core) although their values may change with different domains. The drug delivery is not assumed to be precisely and only to the tumor. Both tumor and normal tissue beds are perfused by the injected artery. However, due to the difference in interstitial pressure distribution, the perfusion is nonuniform, ultimately leading to a heterogeneous drug delivery to be quantified through the present study.

Boundary Condition

The time scale for the simulations is assumed to be much shorter than the time scale for tumor growth, hence the boundaries are taken as fixed. Along the internal boundaries, i.e. the interface of the necrotic core and viable zone, and the viable zone and normal tissue, conditions of continuity of interstitial pressure and fluid flux are imposed. The conditions of continuity of drug concentration and flux are also specified. The interstitial fluid pressure at the outer rim of the normal tissue is specified as the ambient atmospheric pressure, coupled with a no-flux condition at this external boundary.

Table I. Parameters Used for Baseline Simulation: Baseline Parameter Values Are the Default Values Used in the Simulations Unless Specified Otherwise

Parameter	Baseline value (tumor[a])	Baseline value (normal tissue)	Reference
S/V	588.2 cm^{-1}	70.00 cm^{-1}	(5,13,16,27)
K_v	2.10×10^{-11} m/Pa-s	2.70×10^{-12} m/Pa-S	(5,13)
K	3.10×10^{-14} m^2/Pa-s	6.40×10^{-15} m^2/Pa-S	(5,13)
ρ	1,000 kg/m^3	1,000 kg/m^3	[b]
μ	0.00078 kg/m-s	0.00078 kg/m-s	[b]
$1/\kappa$	4.56×10^{16} m^{-2}	2.21×10^{17} m^{-2}	[c]
D	4.84×10^{-9} m^2/s	1.79×10^{-10} m^2/s	(5)[d]
P	5.95×10^{-5} m/s	7.60×10^{-6} m/s	(5)[d]
P_v	2080 Pa (no injection) 2089 Pa (with injection)	2080 Pa (no injection) 2089 Pa (with injection)	(5,13) Appendix A
π_v	2666 Pa	2666 Pa	(5,13)
π_i	2000 Pa	1333 Pa	(5,13)
σ_T	0.82	0.91	(5,13)
σ	0.15	0.15	(5)[c]
K_vS_1/V	0 $(Pa\text{-}s)^{-1}$	4.17×10^{-7} $(Pa\text{-}s)^{-1}$	(6)
P_1	0 Pa	0 Pa	(11)
c	1,000 s	1000 s	[e]
C_{vo}	2.13 mol/m^3	2.13 mol/m^3	Dosage = 50 mg/m^2 Appendix A
T_w	180 s	180 s	(2)

[a] Tumor: viable zone and necrotic core.
[b] Estimated with the properties of water at 37°C.
[c] $\kappa = \mu K$.
[d] Interpolated for molecular weight of 580 g/mol.
[e] Taken as the time scale characteristic of fluid percolation through the interstitial matrix, as reported in Netti *et al.* (3).

Numerical Method

The finite volume method involves the division of the domain into discrete control volumes using the computational grid. The governing equations are then integrated on the individual control volumes to construct algebraic equations for the discrete unknowns. These discretized equations are then solved. Since the governing equations are coupled and solved sequentially, several iterations of each solution loop must be performed to obtain a converged solution. A maximum of 400 iterations are specified for each time step, the size of each time step being 1 min. The SIMPLEC algorithm is used to introduce pressure into the continuity equation. This is a variant of the basic SIMPLE (Semi-Implicit Method for Pressure-Linked Equations) algorithm. Due to the non-linearity of the equation set solved by Fluent/UNS, underrelaxation is needed. A second order accuracy is specified for momentum and species. The Gauss-Siedel smoothing method, in which each point is updated using the most up-to-date values of its neighbors, is used. Unscaled residuals are monitored and checked for convergence. A popular approach to judging convergence is to require that the unscaled residuals drop by three orders of magnitude from their initial values (10).

RESULTS AND DISCUSSION

Simulations were conducted using Fluent/UNS, based on the Finite Volume Method. Simulations were carried out using equations 1 to 6 for fluid transport, coupled with equations 7 to 11 for solute transport. A baseline simulation was first performed. In this simulation, lymphatic drainage was taken to be absent in the tumor zone, but present in the normal tissues of the liver. Intralymphatic pressure was taken to be atmospheric (11). Cellular metabolism and binding kinetics (with DNA) were also not included. Doxorubicin is supplied from the blood vessels. The initial concentration of doxorubicin in blood plasma is calculated based on 50 mg/m^2 for a 70 kg patient (appendix A). The parameters used for the baseline simulation are given in Table I. In searching for the contributions from lymphatic drainage, cellular metabolism and doxorubicin-DNA binding kinetics, computer simulations were conducted by adding/dropping one factor each time and the results were compared with the baseline simulation results and presented in various sections.

Interstitial Fluid Pressure Distributions

The steady-state (before the infusion of drug) pressure distribution for the baseline simulation is shown in Fig. 1a. Interstitial pressure is highest and flat in the center of the tumor with a sharp decrease at the periphery of the tumor. Maximum interstitial pressure occurs in the core, reaching a value of 1.55 kPa, which is close to the value of 1.53 kPa reported by Baxter and Jain (5). Since the pressure is uniformly high in the center of the tumor, pressure-induced convection occurs only within a thin boundary layer between the tumor and the normal tissue. For unit consistency, we have converted all pressure units following the SI unit system (1 Pa = 1 Newton/m^2 = 0.0075 mm Hg).

With the selective delivery of doxorubicin directly into the tumor mass, fluid filtration across the blood vessels is enhanced. Changes in vascular pressure are transmitted to the interstitial pressure, as seen from the mean interstitial pressure in the tumor and core, which follows closely the decaying exponential profile of the vascular pressure (data not shown). This is in accordance to the results obtained by Netti *et al.* (4). Interstitial fluid pressure in the tumor and core reaches a steady state value in about 800 s, as shown in Fig. 2a. This value indicates that the two different mechanisms of fluid transport—transcapillary fluid exchange and interstitial matrix fluid percolation—are involved in the transient process. According to Netti *et al.* (3), the time scale for the former is of the order of magnitude 10 s, and for the latter, 1000 s. Interstitial pressure in the normal tissues takes a longer time of more than 1000 s to reach steady state. The higher resistance of the interstitium to fluid flow of the normal tissue than the tumor accounts for this, as a higher resistance makes it more difficult for fluid to percolate through the interstitial matrix.

The time scale of 1,000 s corresponds to the case of abrupt cessation of tumor blood flow, while the time scale for the process of abrupt increase/decrease of microvascular pressure is about 10 s (3). The actual treatment is between the two extreme cases: the 3-min fluid infusion will impose a rapid increase in blood flow and microvascular pressure, followed by a decay phase depending on the condition of tumor blood flow and the simulation results generated using a decaying

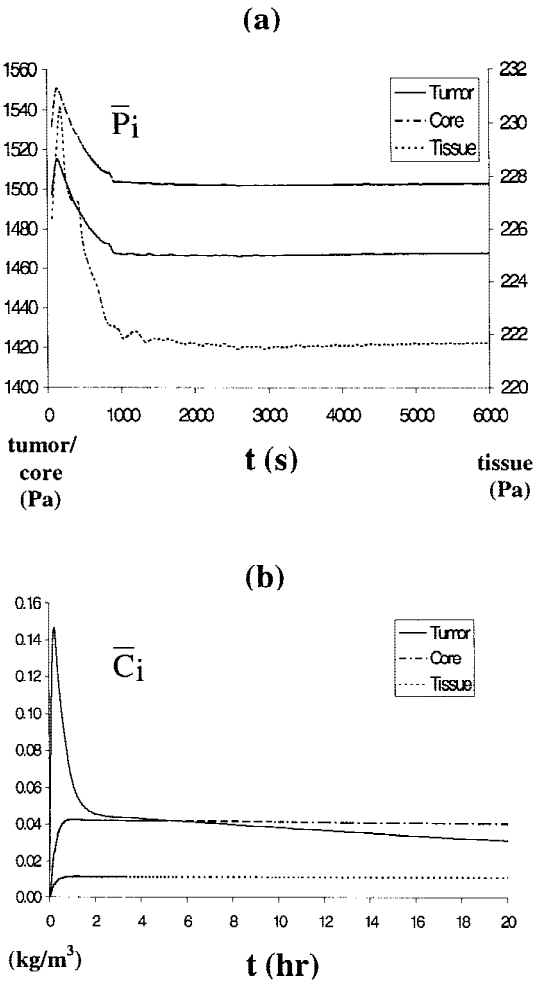

Fig. 2. Temporal evolution of (a) mean interstitial pressure $\overline{P}_i$ and (b) mean interstitial concentration $\overline{C}_i$ profiles of doxorubicin for baseline simulation. Baseline parameter values are given in Table I.

time constant of 1,000 s thus provide a lower bound on the heterogeneity of drug distribution. This is introduced upon considering the time scale of fluid percolation through the porous interstitium. A sensitivity analysis for this decay constant shows that the transient effect becomes less important as the decay time constant is reduced. However, the steady-state flow field will not be changed by varying the value of decay time constant.

Doxorubicin Concentration

Figure 2b shows the change in the mean concentration of doxorubicin in the three different zones with time. Concentration of doxorubicin is highest in the tumor zone, followed by the core and is lowest in the normal tissue. The interstitial concentration in the tumor increases (due to arterial infusion) and decreases sharply in the first hour or so and then subsequently decreases slowly. For the other two zones, concentration increases in the first hour and subsequently decreases very slowly. The rapid decrease in doxorubicin concentration in the tumor is due to the rapid decay of plasma concentrations. Between 0 and 2 h the concentration of doxorubicin in the viable tumor tissue is at least 7-fold higher than in the surrounding tissue. At later times (t > 4 hrs), a concentration differential of at least 2-fold is predicted. These are important concentration differences caused by the higher vascular permeability (about 8-fold) and blood vessel exchange area (S/V, about 8-fold) in the tumor as compared to the surrounding normal tissues (see Table I). The clinical implication of this simulation result is that any treatments applied to sensitize the vascular permeability of tumor tissues can indeed enhance the efficacy of the anticancer treatments.

Referring to Table II (appendix B), there appears to be a good correlation between the drug concentration in the interstitial space of tumor (also following an exponential decay mode) and blood plasma for time >> 1 h. In contrast, the correlation with the normal tissues and necrotic core is not clear. This observation indicates that drug concentration in blood plasma does play a key role in determining the rate of drug delivery to the target tumor at longer times. The toxicity in the surrounding normal tissues, on the other hand, has to be examined through a complete mathematical model.

The only source of doxorubicin into the core is by diffusion from the tumor zone since there are no functional blood vessels in the core. At early time periods, there is little drug in the core. At later time periods, concentration in the core rises beyond the concentration in the tumor as the drug is cleared from the plasma and washed out of the tumor zone. This is known as the reservoir phenomenon (6,12). The accumulation of the drug in the core can be seen from the contour plots of Fig. 3.

Table II. Apparent Rate Constants of Doxorubicin Decay in Plasma for Different Time Periods (26)

Stage	Time period (after injection i.e. $t > T_w$)	C_v^i	k_i (s^{-1})
(i =) 1	0–20 min	C_v^1	2.100×10^{-3}
2	20–40 min	$0.08\ C_v^1$	8.170×10^{-4}
3	40 min–1 h	$0.03\ C_v^1$	1.159×10^{-4}
4	1–2 h	$0.025\ C_v^1$	6.198×10^{-5}
5	2–4 h	$0.02\ C_v^1$	3.996×10^{-5}
6	4–8 h	$0.015\ C_v^1$	2.816×10^{-5}
7	8–48 h	$0.01\ C_v^1$	9.000×10^{-5}

Concentration in the normal tissue is much lower than in the other two zones at all times, partly due to the presence of functional lymphatic vessels, which re-absorb the drug filtered from the blood vessels into the interstitium. Also, the vascular permeability and diffusion coefficients of doxorubicin are smaller in the normal tissues than in the tumor. The low concentration of doxorubicin in the normal tissue is favorable as doxorubicin exhibits toxicity and thus high concentrations in normal tissue are not desired. The distribution of doxorubicin is quite uniform in the tumor zone at all times. Hence, the drug is able to act effectively on the tumor cells.

Effect of Injection Volume

A different volume of injection will result in a different increase in vascular pressure. Following the assumption made in this model, the pressure increase is proportional to the injection volume, for a constant time of injection (refer to equations A.1 and A.2 in appendix A). Different simulations are performed using twice and half the injection volume used in the baseline simulation respectively. It is assumed that the time scale for the decay in vascular pressure remains the same in the order of 1000 s.

An increase in the injection volume may be expected to cause an increase in the concentration of the drug due to enhanced convection caused by the increased transcapillary pressure gradient. However, no significant change is observed in the concentration of doxorubicin in all three zones (data not shown). One possible reason is that the change in vascular pressure caused by the injection of the drug solution is very small. Vascular pressure increase caused by injection of 86.5 ml of solution in the baseline case is 0.5% (refer to appendix A). Increasing the injection volume to twice that of the baseline case results in a vascular pressure increase of only 1%. This increase is not significant enough to bring about an increase in the transvascular pressure gradient to result in higher drug concentrations in the interstitium. In addition, pressure-induced convection for the transport of drug is insignificant as compared to diffusion, as indicated by the small Peclet numbers shown elsewhere in this work.

Effect of Dosage

All simulation results presented in earlier sections refer to the baseline dosage of 50 mg/m^2. To simulate the effect of dosage on the efficacy of drug delivery, the tumor/tissue concentration ratio ($\overline{C}_{tumor}/\overline{C}_{tissue}$) profiles for the dosage of 25 mg/m^2 and 75 mg/m^2 are also shown in Fig. 4, where $\overline{C}_{tumor}$ and $\overline{C}_{tissue}$ are the averaged drug concentration $\overline{C}_i$ for the tumor and normal tissues, respectively. The dosage refers to the mass of drug per unit body surface area (rather than unit volume) of the patient. As expected, a lower dosage of 25 mg/m^2 results in a lower concentration of doxorubicin in all three zones at all times (data not shown). A 50% decrease in dosage yields a nearly proportional reduction (60%) in systemic toxicity in the normal tissues. In contrast, in the tumor zone, this difference in concentration is only significant at early times. The difference drops to within 5 to 10% of the baseline value in about 2 h. This is not surprising as the drug is washed out rapidly from the tumor zone due to its higher

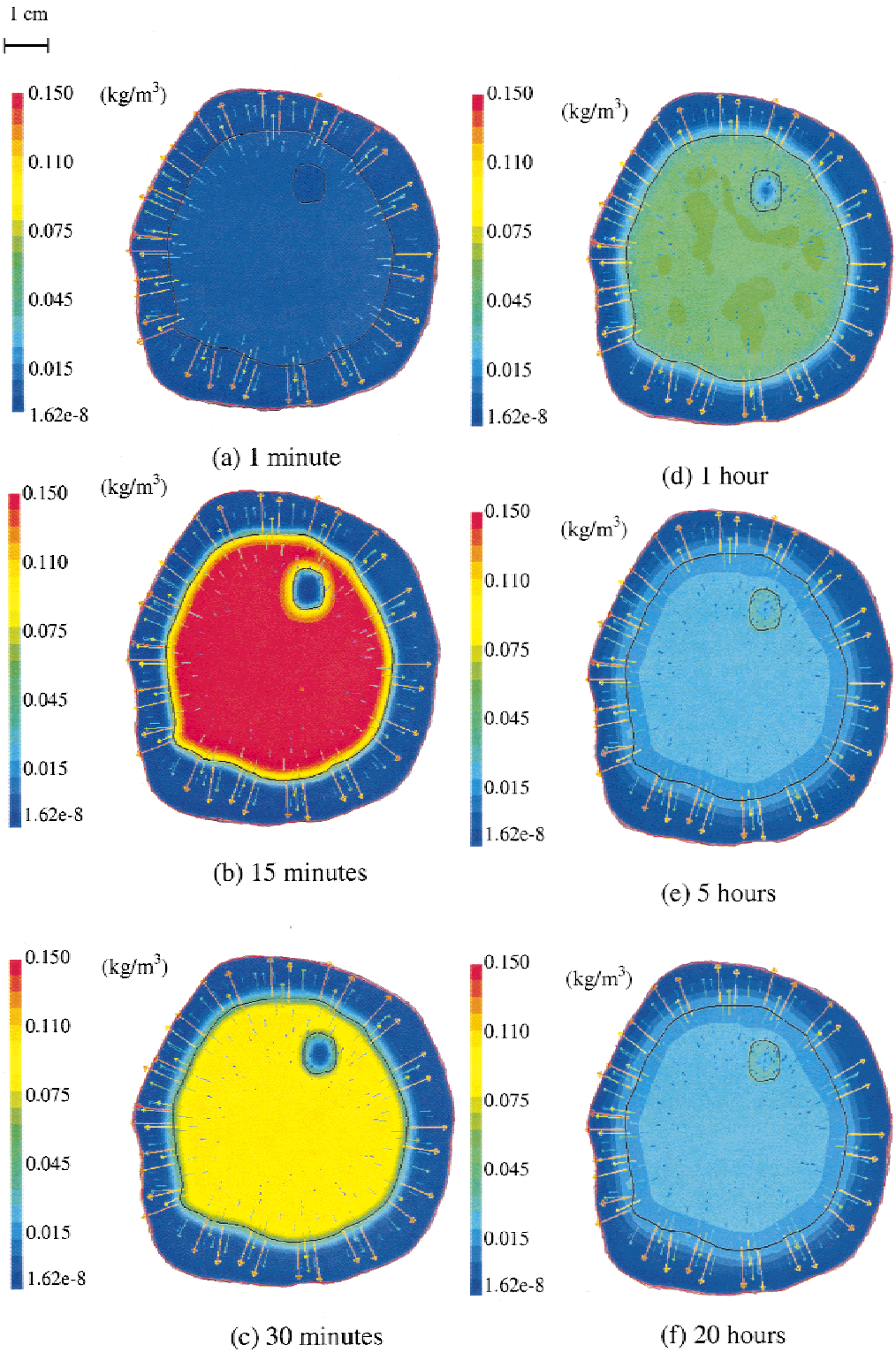

Fig. 3. Spatio-temporal variation in the concentration of doxorubicin (kg/m^3). Baseline parameter values are given in Table I.

diffusivity and vascular permeability, as compared to surrounding normal tissues.

The ratio of tumor/tissue concentrations is an important determinant of drug effect selectivity. Ideally, drug concentration in the tumor should be much higher than in the tissue so that the drug is able to act effectively on the tumor cells and at the same time not exhibit excessive toxic effect on the normal tissue. The simulation result shows that this ratio is higher initially and decreases sharply in the first hour as the drug is rapidly cleared from the tumor zone (Fig. 4). A lower drug dosage gives a higher ratio at all times. Hence, a dosage should be administered according to the solution of an optimization problem in which the drug concentrations are high enough (> therapeutic level) to be able to kill the tumor cells

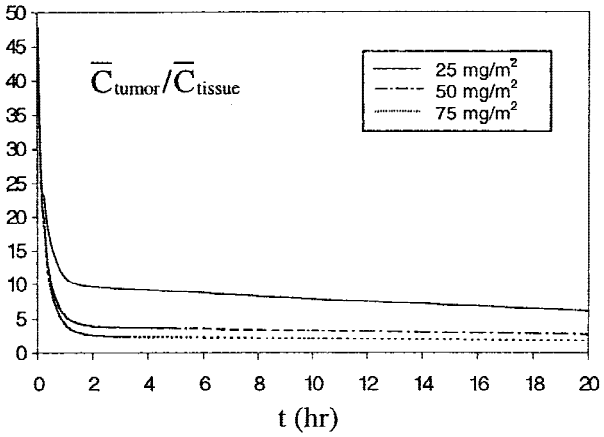

Fig. 4. Ratio of mean doxorubicin concentration in tumor ($\overline{C}_{tumor}$) to tissue ($\overline{C}_{tissue}$) for different dosages. Baseline parameter values are given in Table I.

effectively and yet exhibit low toxicity in the normal tissues (ratio of tumor/tissue concentrations < maximum tolerance of the cytotoxic level).

Effect of Blood Vessel Exchange Area (S/V)

The exchange surface area of blood vessels per unit volume of tumor, S/V, can vary significantly in different tumors, as well as at different growth stages of the same tumor. This effect is simulated by a different S/V ratio in the tumor zone. In earlier sections, the baseline S/V parameters are taken as 588.2 cm^{-1} and 70 cm^{-1} for the tumor and normal tissues, respectively. Figure 5 shows that a 66% decrease in the tumor S/V value (from 588.2 cm^{-1} to 200 cm^{-1}, the normal tissue S/V value remains as 70 cm^{-1}) leads to a 60–85% reduction in drug concentration in all three zones. This is expected since a higher tumor S/V value means a larger surface area available for the drug to diffuse through the capillary wall into the interstitium. A greater blood perfusion in tumor allows more cancerous cells to be killed.

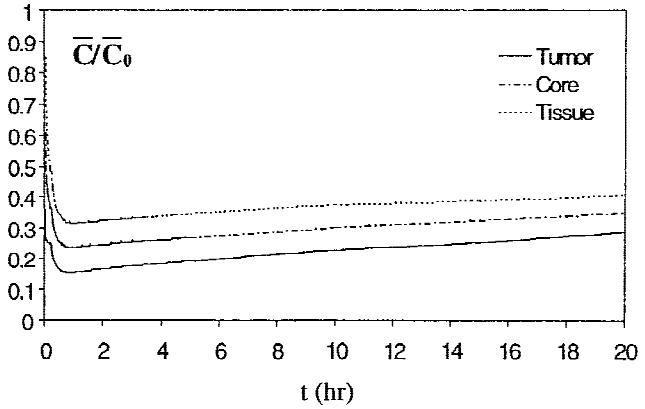

Fig. 5. Effect of S/V ratio. Concentration profiles (normalized with respect to baseline case, $\overline{C}_0$) of doxorubicin in different zones. Baseline parameter values are given in Table I. The baseline S/V parameters are taken as 588.2 cm^{-1} and 70 cm^{-1} for the tumor and normal tissues, respectively. It is shown that a 66% decrease in the tumor S/V value (from 588.2 cm^{-1} to 200 cm^{-1}) leads to a 60–85% reduction in drug concentration in all three zones.

Effect of Lymphatic Drainage

A lymphatic drainage coefficient of 1.04×10^{-6} $(Pa\text{-}s)^{-1}$ in the tumor zone was used, following Baxter and Jain (6). Intralymphatic pressure was taken to be the same as that in the normal tissue, i.e. $P_1 \approx 0$. The maximum mean interstitial pressure in the tumor is lowered by 45% in the presence of lymphatics. It can be expected that the presence of functional lymphatic vessels in the tumor will lower the interstitial concentration of the doxorubicin, as it gets re-absorbed from the interstitium by the lymphatic vessels.

However, the lowering of the drug concentration is not significant (16). Concentrations in all three zones are reduced by less than 0.3%. The slight fluctuations in concentration seen in early times can be attributed to the very small lowering of concentration from the baseline case. To check for the effect of lymphatics on drug concentration, the relative magnitudes of equations 9 and 11 can be compared. Since the transcapillary Peclet number is small (2.0×10^{-5} and 1.95×10^{-4} for tumor and normal tissues, respectively), transport of doxorubicin in the interstitium is largely by diffusion and the convection term (first term) in equation 9 can be ignored. An order of magnitude analysis is done (13),

$$O(P_i - P_l) \approx 10^2 \text{ since } P_l \approx 0;\ O\left[K_l \frac{S_l}{V}(P_i - P_l)\right] \approx 10^{-4};\ O\left(P\frac{S}{V}\right) \approx 1$$

Since the decay of doxorubicin in the plasma is rapid, C_v is low and hence $O(C_v - C_i) = O(C_i)$. There is a difference of 4 orders of magnitude between the transcapillary exchange source term and the lymphatic drainage term. Hence, the presence of lymphatics in the tumor zone does not significantly affect the concentration of doxorubicin in the tumor.

Effect of Cellular Metabolism

Cellular metabolism of doxorubicin also occurs in the tumor and surrounding normal tissues. Doxorubicin undergoes enzymatic reduction to produce several metabolites, the most common of which is doxorubicinol. The enzyme reaction can be described by the following Michaelis-Menten equation:

$$r_i = \frac{r_{max} C_i}{K_m + C_i} \approx \frac{r_{max}}{K_m} C_i = k^* C_i \qquad (12)$$

where r_i is the rate of the reaction, C_i is the interstitial concentration of doxorubicin, r_{max} and K_m are the kinetic constants, k* is the apparent first order rate constant of the cellular metabolism of doxorubicin. The values of r_{max} and K_m for human liver are estimated as (r_{max}, K_m) = (1.59×10^{-7} mol/s, 2.75×10^{-4} mol/l) (14,15,16). It is assumed that the reaction kinetics is the same in the core, tumor and tissue. Since maximum C_i is of the order of magnitude 10^{-1} kg/m^3 (10^{-7} mol/l), which is three orders of magnitude smaller than K_m, the Michaelis Menten expression of equation 12 reduces to a first order rate equation.

The presence of cell metabolism reduces the concentration of doxorubicin in all three zones (Fig. 6). The reduction becomes more significant at later times. The influence of chemical reaction can be shown by the Hatta number (17), given by:

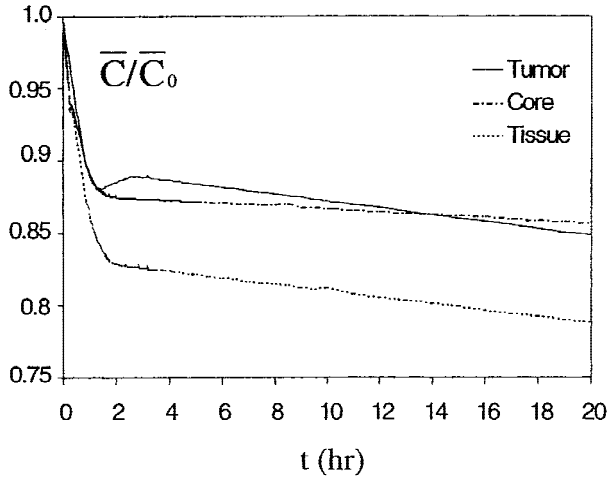

Fig. 6. Effect of cellular metabolism. The values of r_{max} and K_m for human liver are estimated as (r_{max}, K_m) = (1.59×10^{-7} mol/s, 2.75×10^{-4} mol/l) (14,15,16). Concentration profiles (normalized with respect to baseline case, $\bar{C}_0$) of doxorubicin in different zones. Baseline parameter values are given in Table I. The baseline case has no cellular metabolism.

$$M_H = \sqrt{\frac{k^*}{D}}\, L \tag{13}$$

where D is the diffusion coefficient and L is the characteristic length for diffusion, which is taken as half the intercapillary distance of 200 μm, i.e. 100 μm (8).

Using equations 12 and 13, the Hatta numbers for the tumor and tissue zones are found to be 0.27 and 1.39, respectively, indicating that cellular metabolism has a slightly greater influence in the normal tissues than in the tumor (Fig. 6).

Doxorubicin-DNA Binding Kinetics

Doxorubicin is tightly bound to plasma proteins and tissue proteins. This changes its diffusion pattern through the interstitial space, as it diffuses like a protein rather than like a low molecular weight compound. The tight binding to tissue proteins, in particular DNA, also has extensive consequence for tissue accumulation and retention. The intercalation of doxorubicin into DNA and nuclear activation and covalent binding of doxorubicin to DNA are modeled by a reversible binding kinetics given by:

$$\text{Doxorubicin} + \text{DNA} \leftrightarrow \text{B} \tag{14}$$

The apparent rate law is given by (18,19):

$$B_i = k_{on} C_s C_i + \frac{\psi}{\xi}(1 - e^{-t\xi})\, k_{off} \tag{15}$$

where

Ψ = $k_{on} C_{DNA} C_o$
ξ = $k_{on} C_{DNA} + k_{off}$
C_s = DNA binding sites concentration $\cong 7.5 \times 10^{-5}$ [M] (18, 19)
C_i = Interstitial doxorubicin concentration [M]
C_o = Initial (total) doxorubicin concentration [M]
C_{DNA} = DNA base pair concentration $\cong 7.5 \times 10^{-5}$ [M] (18, 19)
k_{on} = association constant = 7.0×10^{-6} [M^{-1} sec] (18, 19)
k_{off} = dissociation constant = 30 [sec^{-1}] (18, 19)

Typical values of the normalized interstitial doxorubicin concentration ($\bar{C}/\bar{C}_0$) are given by: t = 0.2 h, (Tumor, Core, Tissue) = (0.92, 0.93, 0.88); t = 0.5 h, (0.66, 0.78, 0.62); t = 2 h, (0.60, 0.72, 0.43); t = 10 h, (0.55, 0.71, 0.39). Apparently, doxorubicin-DNA binding kinetics can reduce the effective drug concentration by more than 40% in the tumor zone and hence has a more profound effect than the cellular metabolism.

Plasma protein binding of doxorubicin accounts for approximately 75% of the drug in plasma. Despite this high level of plasma protein binding, tissue/plasma doxorubicin ratios range from 10:1 to 500:1 by virtue of the higher affinity of the drugs for DNA as compared with plasma. Because of high binding to protein and DNA, the free-drug pool represents a very small fraction of the drug concentrations measured in both plasma and cells. Bulk of the intracellular drug is in the nucleus, mainly bound to DNA, especially the dGdC-rich regions that are flanked by A:T base pairs. It has been assumed that all the drug within the nucleus is intercalated.

Transvascular movement is by free diffusion of the unionized drug. This is because the molecular size of plasma protein bounded doxorubicin is rather large (e.g. albumin-doxorubicin has a molecular weight of 69,000). Most of them remain in blood plasma rather than get filtered through the walls of blood vessels. Once the free drug reaches the extravascular space, it quickly forms a tissue/doxorubicin complex, mostly bound to DNA. In evaluating the drug distribution in the liver interstitial space, the free doxorubicin concentration should be used as a variable in the mass balance equation (equations 7 and 9). Because the diffusivity of free doxorubicin is much higher than the DNA bounded doxorubicin (justified by the high molecular weight of this complex), the latter form of doxorubicin is essentially immobilized in the nucleus of cells.

Confocal Microscopy Studies

Confocal microscopy studies about the antitumor/antiproliferative activities of doxorubicin-protein/liposome conjugates have been reported extensively in the literature (20,21). However, most of these studies were mainly focused on cellular level and qualitative results. Given the very limited quantitative results available, we have managed to compare our findings only with the results by Wartenburg *et al.* (22) about doxorubicin uptake in prostate tumor spheroids. For large tumor spheroids (diameter ~400 μm), the doxorubicin uptake is limited only to the periphery. In contrast, for small spheroids (diameter ~100 μm), the drug penetration is nearly throughout the whole tumor, shown by the uniform high doxorubicin fluorescence values (recorded by confocal laser scanning microscopy). In both cases, multicellular spheroids were incubated for 60 min with 30 μM doxorubicin. They have found that a prolonged incubation (up to 4 h) did not alter the staining pattern. Since the fluorescence values are not in direct proportion to the drug concentration, one can only obtain qualitative comparison with the model predictions. The limited penetration in large tumor spheroid could be attributed to the unfavorable pressure gradient experienced by quiescent cells, as compared to small spheroids which consist entirely of proliferating cells.

CONCLUSIONS

A two-dimensional model for the delivery of drug to tumors is established. From the baseline simulation, it is found that the time taken for the interstitial pressure in the tumor and core to reach steady state is about 800 s. Mean concentration of doxorubicin is highest in the viable zone of the tumor at early times and in the necrotic core at the later times. Concentration in the normal tissues is the lowest at all times.

Chemotherapy does not discriminate between normal cells and tumor cells per se. Any differential effect on tumor tissue vis-à-vis normal tissue is reflective of: drug delivery to tumor tissues (which is in turn a function of angiogenesis), cell cycling rate, and relative amounts of DNA for drug binding in these two different tissues. Of these three factors, drug delivery is the most amenable to clinical manipulation. It is found that changing the injection volume does not result in significant changes in drug concentration in the tumor, core, and normal tissue. Diffusion is the main mechanism of transport in the interstitium for free doxorubicin molecules. A smaller vascular exchange area results in a lower interstitial drug concentration. Lymphatic drainage in the tumor causes negligible reductions of less than 0.3% in the mean concentrations in all three different zones. Cellular metabolism and DNA binding kinetics also decrease the mean concentrations of drug by about 15 to 40% respectively, as compared to the baseline case.

This model can also be applied to other drug systems with different drug parameter values, as well as different tumor geometry. However, there are limitations to this current analysis. Fluxes from blood vessels are treated as distributed source terms rather than local source terms. A non-uniform blood supply will result in a heterogeneous distribution of drug molecules. Also, the assumption of spatially independent physiological parameters may not hold. The spatial and temporal dependence of these parameters should be considered. In addition for fast-growing tumors the boundaries between the different zones should be modeled as moving instead of fixed boundaries. By incorporating the above considerations, a more accurate description of the actual physiologic model can be obtained.

ACKNOWLEDGMENTS

This work has been supported by National Medical Research Council under the grant number NMRC/0232/1997 (RP970658N). We thank Professor Miranda Yap (Bioprocessing Technology Center, NUS) for many helpful discussions, and Theodore Chen, Chee Seng Teo, Lee Ping Ang, Lai Kian Goh, and Dr. Suryadevara Madhusudana Rao for their technical support on the project.

APPENDIX

A. Calculation of Increase in Vascular Pressure Caused by Injection of Drug

For a bed of uniform parallel capillaries, the relationship between mean capillary flow velocity and capillary density for a given bulk flow rate is given by Renkin (23):

$$\bar{v} = \frac{q\, l_c}{N\, (\pi/4) d_c^{\,2}} \tag{A.1}$$

where $\bar{v}$ is the mean capillary flow velocity, q is the total blood flow per unit tissue volume, N is the number of open capillaries per unit cross sectional area of tissue, d_c is the capillary diameter, and l_c is the average depth of tissue traversed by the capillary, i.e. length of capillary. These parameters are obtained from Renkin (23) as (N, l_c, d_c, μ_b) = (1000 mm^{-2}, 1 mm, 10 μm, 2.0 cP).

The pressure-flow relationship for flow of blood in capillaries can be represented by the Hagen-Poiseulle's equation (24):

$$\Delta P = \frac{8Q\mu_b\, l_c}{\pi\, r^4} = \frac{8\bar{v}\mu_b\, l_c}{r^2} \tag{A.2}$$

where Q is the bulk flow rate and μ_b is the apparent viscosity of blood in the capillary. Injection of the drug will lead to an increase in the mean capillary flow velocity and hence the mean capillary pressure will increase. This increase is calculated by the infusion speed of fluid into parallel capillaries by equation A.2, assuming the capillaries as series of rigid microvessels. The increase in bulk flow rate of blood per unit volume of tissue (i.e. Δq) due to the injection of drug is calculated from the administration regimen of the drug. From (2), dosage of doxorubicin is 50 mg/m^2. Body surface area (BSA) is determined from the following formula (25):

$$\text{BSA } (m^2) = \left(\frac{\text{Weight in kg}}{70\text{ kg}}\right)^{0.73} (1.73\ m^2) \tag{A.3}$$

For a 70 kg patient, dosage of doxorubicin is 86.5 mg. This amount of drug is dissolved in saline in a 1:1 mass to volume ratio (2). Time of injection is 3 min, giving a bulk flow rate of 0.48 ml/s. Hence, for a tumor volume of 440 cm^3, $\Delta q = 0.0011\ s^{-1}$. Using equations (A.1) and (A.2), the increase in mean capillary pressure P_v is found to be 9.0 Pa i.e. 0.5%.

B. Calculation of Doxorubicin Concentration in Blood Plasma C_v

The plasma pharmacokinetics of doxorubicin was obtained from the data of Robert *et al.* (26). The disappearance of doxorubicin follows a tri-exponential decay characterized by three successive half-lives of 3 to 5 min, 1 to 2 h, and 24 to 36 h. The decrease in doxorubicin concentration can be divided into different stages, corresponding to different time periods, each following an exponential decay of the form:

$$C_v = C_v^i \exp(-k_i\, t) \tag{B.1}$$

where C_v^i is the initial concentration at the beginning of each stage and k_i is the apparent rate constant of that stage. The values of C_v^i and k_i are tabulated in Table II. During the period of injection, C_v increases exponentially with time. At the end of the injection period ($t = T_w$), which is also the beginning of the first stage, the concentration of doxorubicin in the plasma is given by:

$$C_v^1 = \frac{C_{vo}}{T_w k_1}\left[1 - \exp(-k_1 T_w)\right] \tag{B.2}$$

where C_{vo} is the initial concentration of drug injected, T_w is the time period of injection (~3 min), and k_1 is the initial

apparent rate constant. The temporal evolution of the plasma drug concentration is shown in Table II.

REFERENCES

1. R. Yamada, K. Kishi, M. Terada, T. Sonomura, and M. Sato. Transcatheter arterial chemoembolization for unresectable hepatocellular carcinoma. In T. Tobe (ed.), *Primary Liver Cancer in Japan*, Springer-Verlag, Tokyo and New York, 1992 pp. 259–271.
2. L. B. Grochow and M. Matthew. *A Clinician's Guide to Chemotherapy Pharmacokinetics and Pharmacodynamics*, Williams & Wilkins, Baltimore, 1998.
3. P. A. Netti, L. T. Baxter, Y. Boucher, R. Skalak, and R. K. Jain. Time-dependent behaviour of interstitial fluid pressure in solid tumors: Implications for drug delivery. *Cancer Res.* **55**:5451–5458 (1995).
4. P. A. Netti, L. M. Hamberg, J. W. Babich, D. Kierstead, W. Graham, G. J. Hunter, G. L. Wolf, A. Fischman, Y. Boucher, and R. K. Jain. Enhancement of fluid filtration across tumor vessels: Implications for delivery of macromolecules. *Proc. Natl. Acad. Sci. USA* **96**:3137–3142 (1999).
5. L. T. Baxter and R. K. Jain. Transport of fluid and macromolecules in tumors. I role of interstitial pressure and convection. *Microvas. Res.* **37**:77–104 (1989).
6. L. T. Baxter and R. K. Jain. Transport of fluid and macromolecules in tumors. II role of heterogeneous perfusion and lymphatics. *Microvas. Res.* **40**:246–263 (1990).
7. L. T. Baxter and R. K. Jain. Transport of fluid and macromolecules in tumors. III role of binding and metabolism. *Microvas. Res.* **41**:5–23 (1991).
8. L. T. Baxter and R. K. Jain. Transport of fluid and macromolecules in tumors. IV a microscopic model of the perivascular distribution. *Microvas. Res.* **41**:252–272 (1991).
9. F. E. Curry. Mechanics and thermodynamics of transcapillary exchange. In S. R. Geiger, E. M. Renkin, and C. C. Michel (eds.), *Handbook of Physiology Section 2—The Cardiovascular System IV, Part 1*, American Physiological Society, Bethesda, Maryland, 1984 pp. 309–374.
10. *Fluent/UNS & Rampant Version 4.2 User's Guide Volumes 1–4*, Fluent, Inc. 1997.
11. B. W. Zweifach and H. H. Lipowsky. Pressure-flow relations in blood and lymph microcirculation. In S. R. Geiger, E. M. Renkin, and C. C. Michel (eds.), *Handbook of Physiology Section 2—The Cardiovascular System IV, Part 1*, American Physiological Society, Bethesda, Maryland, 1984 pp. 251–308.
12. R. K. Jain and J. Wei. Dynamics of drug transport in solid tumors: Distributed parameter model. *J. Bioeng.* **1**:313–330 (1977).
13. C. H. Wang, J. Li, C. S. Teo, and T. Lee. The delivery of BCNU to brain tumors. *J. Controll. Release* **61**:21–41 (1999).
14. H. Loveless, E. Arena, R. L. Felsted, and N. R. Bachur. Comparative mammalian metabolism of adriamycin and daunorubicin. *Cancer Res.* **38**:593–598 (1978).
15. S. Kalyanasundaram, V. D. Calhoun, and K. W. Leong. A finite element model for predicting the distribution of drugs delivered intracranially to the brain. *Am. J. Physiol.* **273**:R1810–R1821 (1997).
16. Y. M. F. Goh. Simulation of drug delivery to hepatoma, B. Eng. Thesis, Department of Chemical and Environmental Engineering, National University of Singapore (1999).
17. J. R. Welly, C. E. Wicks, and R. E. Wilson. *Fundamentals of Momentum, Heat and Mass Transfer*, John Wiley and Sons, New York, 1984.
18. V. Rizzo, N. Sacchi, and M. Menozzi. Kinetic studies of anthracycline-DNA interaction by fluorescence stopped flow confirm a complex association mechanism. *Biochemistry* **28**:274–282 (1989).
19. M. Yang, H. L. Chan, W. Lam, and W. F. Fong. Cytotoxicity and DNA binding characteristics of dextran-conjugated doxorubicins. *Biochim. Biophys. Acta* **1380**:329–335 (1998).
20. F. Gabor, I. Haberl, M. Wirth, K. Richter, G. Theyer, G. Baumgartner, E. Wenzl, and G. Hamilton. *In vitro* antitumor activity of MIC2 protein-doxorubicin conjugates. *Int. J. Oncology* **9**:527–531 (1996).
21. R. Kirshna, M. St-Louis, and L. D. Mayer. Increased intracellular drug accumulation and complete chemosensitization achieved in multidrug-resistant solid tumors by co-administering valspodar (PSC 833) with sterically stabilized liposomal doxorubicin. *Int. J. Cancer* **85**:131–141 (2000).
22. M. Wartenberg, C. Frey, H. Diedershagen, J. Ritgen, J. Hescheler, and H. Sauer. Development of an intrinsic P-glycoprotein-mediated doxorubicin resistance in quiescent cell layers of large, multicellular prostate tumor spheroids. *Int. J. Cancer* **75**:855–863 (1998).
23. E. M. Renkin. Control of Microcirculation and Blood-tissue Exchange. In S. R. Geiger, E. M. Renkin, and C. C. Michel (eds.), *Handbook of Physiology Section 2—The Cardiovascular System IV, Part 2*, American Physiological Society, Bethesda, Maryland, 1984 pp. 627–688.
24. R. K. Jain. Determinants of tumor blood flow: A review. *Cancer Res.* **48**:2641–2658 (1988).
25. E. M. Winter. *Basic Clinical Pharmacokinetics*, Applied Therapeutics, Inc., San Francisco, 1980.
26. J. Robert, N. B. Bui, and P. Vrignaud. Pharmacokinetics of doxorubicin in sarcoma patients. *Euro. J. Clin. Pharmacol.* **31**:695–699 (1987).
27. D. E. Hilmas and E. L. Gillette. Morphometric analyses of the microvasculature of tumor during growth and after x-irradiation. *Cancer* **33**:103–110 (1974).